European Review for Medical and Pharmacological Sciences 2020; 24: 4348-4360

Hsa_circ_0124055 and hsa_circ_0101622 regulate proliferation and apoptosis in thyroid cancer and serve as prognostic and diagnostic indicators

J.-W. SUN, S. QIU, J.-Y. YANG, X. CHEN, H.-X. LI

Department of Breast and Thyroid Surgery, The First People's Hospital of Yunnan Province & Affiliated Hospital of Kunming University of Science and Technology, Kunming, Yunnan Province, P.R. China

Abstract. – OBJECTIVE: Recent studies have corroborated that circular RNAs (circRNAs) as endogenous noncoding RNAs gain research interest in carcinogenesis, functioning as prognostic and diagnostic biomarkers and therapeutic targets. The present study is aimed to determine whether circRNAs could serve as prognostic and diagnostic biomarkers to predict thyroid carcinoma.

MATERIALS AND METHODS: High-throughput sequencing analysis was conducted to detect circRNAs expression profile in thyroid cancer. Reverse transcription-quantitative polymerase chain reaction (RT-qPCR) measurement was utilized to validate circRNAs expression in blood and tissue specimens. Kaplan-Meier method and receiver operating characteristic (ROC) curves and the area under the ROC curve (AUC) were used to assess whether circRNAs could function as prognostic and diagnostic biomarkers of thyroid cancer, respectively.

RESULTS: Hsa_circ_0124055 and hsa_circ_0101622 as the most conspicuous biomarkers were significantly increased in tumor tissues and plasma of thyroid cancer patients. High hsa_circ_0124055 or hsa_circ_0101622 expression exhibited shorter overall survival. Our findings also provided strong evidence that plasma hsa_circ_0124055 (AUC = 0.836, 95% CI: 0.763-0.908, $p<0.001$) and hsa_circ_0101622 (AUC = 0.805, 95% CI: 0.727-0.883, $p<0.001$) could be used as diagnostic markers for thyroid cancer, and hsa_circ_0124055 combined with hsa_circ_0101622 could provide a more powerful diagnostic value (AUC = 0.911, 95% CI: 0.859-0.962, $p<0.001$) than the use of hsa_circ_0124055 or hsa_circ_0101622 alone. Furthermore, the knockdown of hsa_circ_0124055 or hsa_circ_0101622 exhibited a significant anti-proliferative and pro-apoptotic activity of thyroid cancer cells *in vivo* and *in vitro*.

CONCLUSIONS: Both hsa_circ_0124055 and hsa_circ_0101622 could facilitate the prognosis and diagnosis of thyroid cancer, and function as the therapeutic targets for clinical practice.

Key Words:
CircRNAs, Papillary thyroid cancer, Diagnosis, Prognosis.

Introduction

Thyroid cancer is one of the most common malignant tumors amongst the endocrine cancers and ranks ninth for incidence, with 567,000 cases worldwide[1,2]. In recent decades, the incidence of thyroid cancer has been increasing in many countries, which is attributed to the increased diagnosis of papillary thyroid carcinoma (PTC), accounting for approximately 80% of all patients with thyroid cancer[3]. Therefore, it is very meaningful to investigate the prognostic and diagnostic biomarkers to improve the clinical outcomes of thyroid cancer patients.

With the development of next-generation sequencing and bioinformatics algorithm, the abundance of non-coding RNAs, such as microRNAs (miRNAs), long non-coding RNAs (lncRNAs), and circular RNAs (circRNAs), is implicated in various developmental stages in mammal and pathological conditions[4-7]. Among these noncoding transcripts, circRNAs represent a novel class of endogenous non-coding RNAs and generate by back-splicing with covalently closed loop structures, which endows them a higher stabilization and can blunt circRNAs to exonucleases-induced degradation[8]. CircRNAs can function as prognostic and diagnostic indicators in various diseases, including cancers, which may be due to their conservation, stability, abundance and tissue specificity[9-12]. In PTC tissues, 98 circRNAs are significantly differentially expressed, suggesting that the dysregulation of circRNAs may play a vital role in the pathogenesis of thyroid

Corresponding Author: Jian-Wei Sun, MD; e-mail: 13888371953@126.com

cancer[13]. Bioinformatics analysis reveals an important regulatory mechanism of circRNAs that function as competing endogenous RNAs *via* the circRNA-miRNA-gene regulatory network[14-17]. The findings suggest that circRNAs provide potential biomarkers and therapeutic targets for the management of thyroid cancer.

The present study utilized high-throughput sequencing analysis to investigate the circRNA profile in thyroid cancer tissues and adjacent non-tumor tissues. The results demonstrated that hsa_circ_0124055 and hsa_circ_0101622 were significantly elevated in thyroid cancer tissues compared with those in adjacent non-tumor tissues. Hsa_circ_0124055 and hsa_circ_0101622 are located in chr3:49514281-49548252 and chr14:31775937-31858211, the spliced sequence length are 620 nt 4194 nt, and their associated-gene symbols are dystroglycan 1 (DAG1) and heat repeat containing 5A (HEATR5A), respectively. Moreover, the prognostic and diagnostic significance of hsa_circ_0124055 and hsa_circ_0101622 were explored in our cohort. *In vivo* and *in vitro* experimental measurements were performed to determine the association between thyroid cancer cell growth and hsa_circ_0124055 or hsa_circ_0101622 expression levels.

Material and Methods

Clinical Specimens

66 thyroid cancer patients (50 papillary thyroid carcinoma, 13 follicular thyroid carcinoma, and 3 undifferentiated thyroid carcinoma) and 66 healthy subjects were recruited in the First People's Hospital of Yunnan Province & Affiliated Hospital of Kunming University of Science and Technology from January 2009 to December 2012. Clinicopathological characteristics of 66 patients with thyroid cancer were shown in Table I. 66 pairs of thyroid cancer tumor tissues and adjacent non-tumor tissues were collected from thyroid cancer patients who underwent curative-intent surgery. 10 ml peripheral whole blood was also obtained from each pre-operative and post-operative thyroid cancer patient and healthy subject using ethylenediaminetetraacetic acid (EDTA)-containing tubes (Becton, Dickinson and Company, Franklin Lakes, NJ, USA), and plasma was separated from peripheral whole blood using centrifuge (x2000 g, 3 min; Thermo Fisher Scientific, Inc., Waltham, MA, USA). All thyroid cancer patients were not subjected to pre-operative radiotherapy or chemotherapy and they were diagnosed with histopathological evaluation. Written informed consent was obtained from all the participants before blood samples collection or operative treatment. The study protocol was approved by the Ethics Committee of the First People's Hospital of Yunnan Province & Affiliated Hospital of Kunming University of Science and Technology (Kunming, China).

Enzyme-Linked Immunosorbent Assay (ELISA)

Serum carcinoembryonic antigen (CEA) and thyroglobulin (Tg) were measured using commercial kits from (Elabscience Biotechnology Co.,

Table I. Clinicopathological characteristics of 66 patients with thyroid cancer.

Characteristics	Subtype	Patients (No.; %)
Gender	Male	21 (31.8)
	Female	45 (68.2)
Age	> 45	31 (47.0)
	≤ 45	35 (53.0)
Histological type	Papillary thyroid carcinoma	50 (75.8)
	Follicular thyroid carcinoma	13 (19.7)
	Undifferentiated thyroid carcinoma	3 (4.5)
Focus type	Unifocal	41 (62.1)
	Multifocal	20 (30.3)
	Unknown	5 (7.6)
CEA (ng/mL)	> 5	22 (33.3)
	≤ 5	44 (66.7)
Tg (ng/mL)	> 100	35 (53.0)
	≤ 100	31 (47.0)

CEA, carcinoembryonic antigen; thyroglobulin, Tg.

Ltd, Wuhan, Hubei Province, China), according to the manufacturer's instructions.

High-Throughput Sequencing

Total RNA was extracted using TRIzol (Invitrogen; Thermo Fisher Scientifc, Inc., Waltham, MA, USA). Ribosomal RNAs and linear RNAs were removed from total RNAs using the Ribo-Zero Magnetic Kit and RNase R (Epicentre Technologies, Madison, WI, USA), respectively. The paired-end sequencing library was constructed according to TruSeq™ Stranded Total RNA Library Prep Kit assay (Illumina, San Diego, CA, USA). RNA sequences were identified using the HiSeq 4000 sequencer platform (Illumina, San Diego, CA, USA). Differentially expressed circRNAs were selected by *p*-value less than 0.001, false discovery rate (FDR) ≤ 0.001 and $|\text{Log}_2\text{fold change}| \geq 1$, and the analysis methods were performed as previously described[18,19].

RT-qPCR

RT-qPCR was conducted to validate differentially expressed circRNAs which were filtrated by high-throughput sequencing analysis. PrimeScript® RT kit (TaKaRa, Dalian, Liaoning Province, China) and SYBR Premix® Ex Taq™ Kit (TaKaRa, Dalian, Liaoning Province, China) were used to perform RT-qPCR analysis by Applied Biosystems 7300 Real Time-PCR System (Thermo Fisher Scientific, Inc., Waltham, MA, USA). The relative expression levels of mRNA were calculated using the $2^{-\Delta\Delta Cq}$ method[20] and normalized to U6. The PCR primers were used as follows: hsa_circ_0124055: forward primer 5'-AGTGCAGCCATCTGGGATAG-3' and reverse primer 5'-TTCGAGTGACCATTCCAACA-3'; hsa_circ_0101622: forward primer 5'-GAAGTGCAGAAGCAGCCTCAC-3' and reverse primer 5'-AGGAATCCTGAACTCCCACG-3'; U6: forward primer 5'- CTCGCTTCGGCAGCACA-3' and reverse primer 5'-AACGCTTCACGAATTTGCGT-3'.

Cell Culture

All cell lines were utilized in our research obtaining from the American Type Culture Collection (ATCC, Manassas, VA, USA). Nthy-ori3-1 cells were cultured in CM-H023 medium (Procell, Wuhan, Hubei Province, China), and thyroid cancer cell lines, including K-1, TPC-1, B-CPAP and CAL-62, were cultured in RPMI-1640 medium (Life Technologies, Carlsbad, CA, USA) supplemented with penicillin G (100 U/ml), streptomycin (100 μg/ml) and 10% fetal bovine serum (FBS, Life Technologies, Carlsbad, CA, USA) with 5% CO_2 atmosphere at 37°C.

Cell Counting Kit-8 (CCK-8) Assays

CCK-8 (Dojindo Laboratories, Kumamoto, Japan) kit was used to analyze cell proliferation every 24 h for three days. Transfected cells (1×10^4 cells/well) were seeded into 96-well plates and cultured at 37°C with 5% CO_2. After incubated with CCK-8 (10 μL) for 2 h, the absorbance was measured at 450 nm a spectrophotometer (Thermo Fisher Scientific, Inc., Waltham, MA, USA).

Cell Apoptosis

Annexin V-fluorescein isothiocyanate/propidium iodide (Annexin V-FITC/PI) (Invitrogen, Carlsbad, CA, USA) double staining was performed to measure cell apoptosis rate. The apoptosis of transfected cells was measured by flow cytometry analysis (FACScan, BD Biosciences, San Jose, CA, USA). The apoptotic cell proportion was analyzed by CELL Quest 3.0 software (BD Biosciences, San Jose, CA, USA).

Cell Transfection

The small interfering RNAs (si-RNAs) to specifically repress hsa_circ_0124055 and hsa_circ_0101622 was synthesized by RiboBio (Guangzhou, Guangdong Province, China). K-1 and TPC-1 cells were transfected with corresponding plasmids for 48 h at 37°C using Lipofectamine 2000 (Invitrogen, Thermo Fisher Scientifc, Inc., Waltham, MA, USA).

Tumor Growth In Vivo

TPC-1 cells (1×10^7/0.1 mL) were transfected with si-Con, si-0124055, and si-0101622 and were then implanted subcutaneously into 4 week-old male nude mice (n = 6 in each group, Beijing HFK Bio-Technology Co., LTD., Beijing, China). Tumor volume and weight were measured when mice were sacrificed at 5 weeks after cell implantation. The animal experiments were approved by the Ethics Committee of the First People's Hospital of Yunnan Province & Affiliated Hospital of Kunming University of Science and Technology (Kunming, China).

Statistical Analysis

Data were presented as mean ± standard deviation (SD). Statistical analysis was performed using IBM SPSS Statistics Version 19.0 (SPSS Inc., Chi-

cago, IL, USA). Chi-Square (χ^2) tests were used to evaluate the differences between the clinical characteristics and circRNAs expression. The student *t*-test was used to analyze two-group differences. Inter-group differences were analyzed by one-way analysis of variance, followed by Tukey's post hoc analysis. Survival analysis was performed using the Kaplan-Meier method with the log-rank test applied for comparison. Receiver operating characteristic (ROC) curves and the area under the ROC curve (AUC) were used to assess the ability to use plasma hsa_circ_0124055 and hsa_circ_0101622 as diagnostic biomarkers of thyroid cancer. The binary logistic regression analysis was used to combine the expression level of hsa_circ_0124055 and hsa_circ_0101622 as combined diagnostic markers for thyroid cancer. The maximum value of the Youden index was used as a criterion for selecting the optimum cutoff point. $p < 0.05$ was considered to indicate a statistically significant difference.

Results

Differentially Expressed CircRNAs Analysis

Using high-throughput sequencing circRNAs expression profile was analyzed in five pairs of thyroid cancer tissues and adjacent non-tumor tissues. The results demonstrated that a total of 231 circRNAs were significantly abnormally expressed in thyroid cancer specimens as compared to adjacent non-tumor tissues (Figure 1A), based on screening criteria $p < 0.001$, FDR ≤ 0.001 and $|\text{Log}_2\text{fold change}| \geq 1$. Among these circRNAs, 98 circRNAs were significantly downregulated and 133 circRNAs were significantly upregulated in thyroid cancer specimens compared with adjacent non-tumor tissues (Figure 1A). In addition, the heatmap exhibited the top six differentially expressed circRNAs, including hsa_circ_0124055, hsa_circ_0101622, hsa_circ_0101174, hsa_circ_0103215, hsa_circ_0102450, and hsa_circ_0103123 (Figure 1B). The expression levels of hsa_circ_0124055 and hsa_circ_0101622 were significantly higher in thyroid cancer specimens than those in the adjacent non-tumor tissues, while hsa_circ_0101174, hsa_circ_0103215, hsa_circ_0102450 and hsa_circ_0103123 were significantly lower in thyroid cancer specimens than those in the adjacent non-tumor tissues (Figure 1C). Furthermore, the genetic information of the top six differentially expressed circRNAs was summarized in Figure 1C.

Hsa_circ_0124055 and Hsa_circ_0101622 were Associated with Poor Prognosis of Thyroid Cancer Patients

To corroborate the results from high-throughput sequencing, RT-qPCR analysis was performed to explore the expression levels of hsa_circ_0124055 and hsa_circ_0101622 in 66 pairs of thyroid cancer tissues and adjacent non-tumor tissues. The RT-qPCR data was consistent with results from high-throughput sequencing (Figure 2A and 2B). 66 TH thyroid cancer patients were divided into two sub-groups (high expression and low expression groups) according to fold changes of circRNAs greater than 1. High expression of hsa_circ_0124055 or hsa_circ_0101622 in thyroid cancer patients was significantly correlated with larger tumor sizes, poorer TNM or histological grades and lymph node metastases. However, the expression levels of hsa_circ_0124055 or hsa_circ_0101622 had no evident correlation with gender and age in thyroid cancer patients (Table II). Kaplan-Meier analysis revealed a significant association between poor prognosis and larger tumor sizes, poorer TNM or histological grades and lymph node metastases in thyroid cancer patients (Figure 3). However, gender and age did not influence the overall survival prognosis of thyroid cancer patients (Figure 3). Notably, patients with high expression levels of hsa_circ_0124055 or hsa_circ_0101622 showed shorter overall survival than patients with low expression (Figure 3).

Hsa_circ_0124055 and Hsa_circ_0101622 Could Serve as Diagnostic Biomarkers for Thyroid Cancer Screening

To determine whether hsa_circ_0124055 and hsa_circ_0101622 could function as biomarkers for the diagnosis of thyroid cancer, we measured the expression levels of hsa_circ_0124055 and hsa_circ_0101622 in plasma from 65 thyroid cancer patients and 65 healthy volunteers. The expression levels of hsa_circ_0124055 and hsa_circ_0101622 were observed to be significantly upregulated in the plasma of thyroid cancer patients compared with that of healthy volunteers (Figure 4A and 4B). Previous study documents that non-coding RNAs are primarily released or leaked from cancerous lesions, which supports the hypothesis that non-coding RNAs can revert to normal levels after excisional operation[21]. To explore whether plasma circRNAs were susceptible to neoplasm growth, RT-qPCR analysis was carried out to detect hsa_circ_0124055 and hsa_circ_0101622 levels in the plasma of thyroid cancer patients before

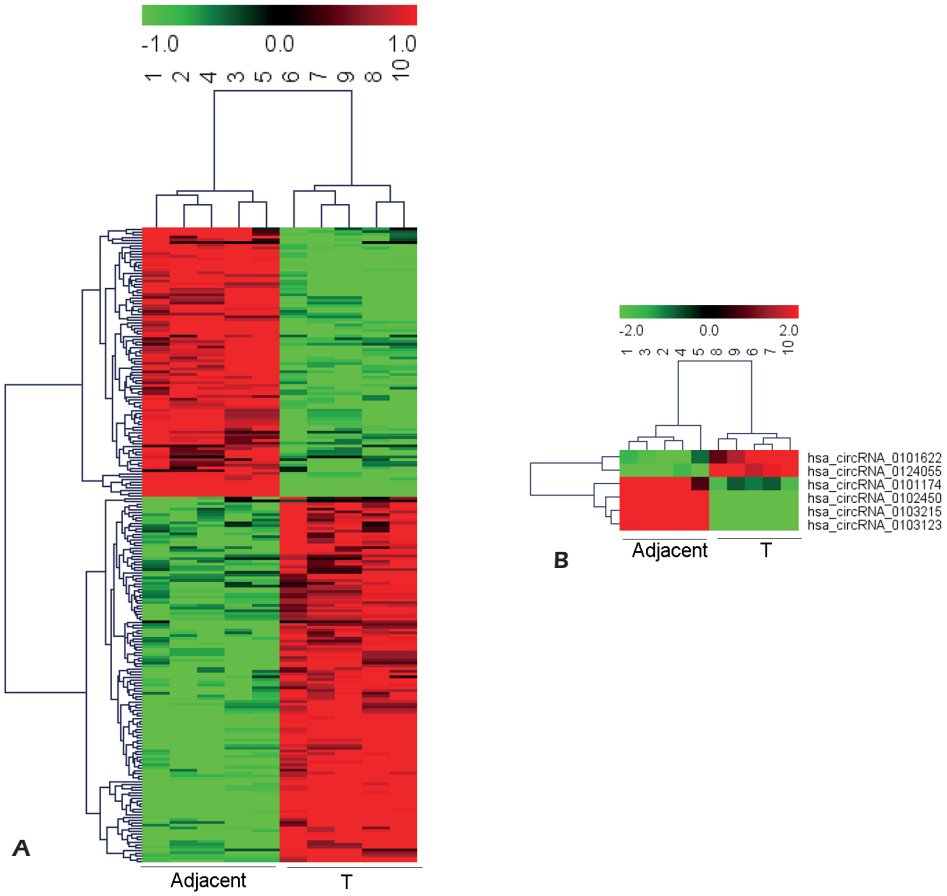

C

circRNA ID	Gene symbol	Spliced length	Position	Log2FC (T/Adjacent)	*p*-value
hsa_circ_0124055	DAG1	620	chr3:49514281-49548252	4.44	< 0.001
hsa_circ_0101622	HEATR5A	4194	chr14:31775937-31858211	3.75	< 0.001
hsa_circ_0101174	EML1	923	chr14:100367265-100384186	-3.73	< 0.001
hsa_circ_0103215	UBE3A	12250	chr15:25638892-25657118	-4.77	< 0.001
hsa_circ_0102450	GPHN	330	chr14:67490349-67567628	-4.95	< 0.001
hsa_circ_0103123	TUBGCP5	4768	chr15:22873201-22877969	-4.97	< 0.001

Figure 1. Differentially expressed circRNAs analysis. Using high-throughput sequencing analysis, circRNAs expression profile is analyzed in five pairs of thyroid cancer and adjacent non-tumor tissues, and a total of 231 circRNAs are significantly abnormally expressed in thyroid cancer specimen as compared to adjacent non-tumor tissues (**A**). Heatmap represents top six differentially expressed circRNAs (**B**). The genetic information of top six differentially expressed circRNAs was summarized (**C**).

and 14 days after surgery. Our findings uncovered the significant decline of hsa_circ_0124055 and hsa_circ_0101622 in plasma of thyroid cancer patients with tumorectomy (Figure 4C and 4D). The stability of circRNAs in plasma is a prerequisite for utilizing them as diagnostic markers. Therefore, we determined the stability of hsa_circ_0124055 and hsa_circ_0101622 under room temperature and freeze-thaw conditions. Hsa_circ_0124055 and hsa_circ_0101622 expression had no evident

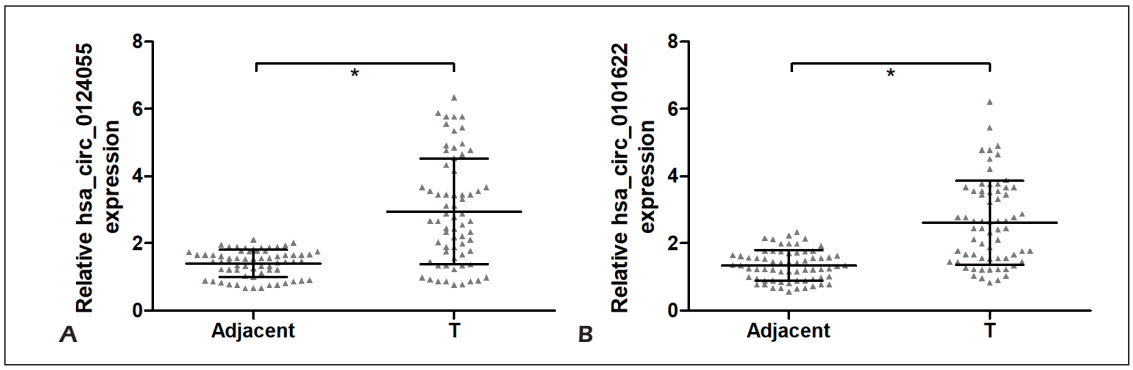

Figure 2. Hsa_circ_0124055 and hsa_circ_0101622 expression levels were up-regulated in thyroid cancer tissues. RT-PCR analysis is performed to measure the expression levels of hsa_circ_0124055 (**A**) and hsa_circ_0101622 (**B**) in 66 pairs of thyroid cancer specimen and adjacent non-tumor tissues. *p<0.05.

change in room temperature before 18 h, but then, significantly declined at 24 h compared with 0 h (Figure 4E and 4F). Data presented in Figure 4G and 4H indicated that hsa_circ_0124055 and hsa_circ_0101622 in plasma remained stable in five freeze-thaw cycles. The results suggest that hsa_circ_0124055 and hsa_circ_0101622 are suitable for serving as diagnostic markers.

To explore whether hsa_circ_0124055 and hsa_circ_0101622 could serve as the diagnostic biomarkers for thyroid cancer, and ROC with AUC was utilized to evaluate the diagnostic significance. The ROC curve showed the diagnostic value of hsa_circ_0124055 (AUC = 0.836, 95% CI: 0.763-0.908, $p < 0.001$; sensitivity 0.712; specificity 0.939; Figure 5A and Table III); hsa_circ_0101622 (AUC = 0.805, 95% CI: 0.727-0.883, $p < 0.001$; sensitivity 0.712; specificity 0.894; Figure 5B and Table III). The AUC was markedly increased after combining with hsa_circ_0124055 and hsa_circ_0101622 (AUC = 0.911, 95% CI: 0.859-0.962, $p < 0.001$; sensitivity 0.894; specificity 0.818; Figure 5C and Table III).

Knockdown of Hsa_circ_0124055 and Hsa_circ_0101622 Led to Thyroid Cancer Cell Growth Blockage and Apoptosis

Based on the above findings, we speculated that the upregulation of hsa_circ_0124055 and

Table II. Correlation between clinicopathological variables and the expression of hsa_circ_0124055 and hsa_circ_0101622.

Variables	No.	hsa_circ_0124055 expression			hsa_circ_0101622 expression		
		Low (n = 33)	High (n = 33)	*p*-value	Low (n = 38)	High (n = 28)	*p*-value
Gender				0.447			0.474
Male	25	11	14		13	12	
Female	41	22	19		25	16	
Age (years)				0.802			0.782
≤ 45	27	13	14		15	12	
> 45	39	20	19		23	16	
Tumor size (cm)				0.002			0.003
≤ 2	44	28	16		31	13	
> 2	22	5	17		7	15	
TNM				0.007			0.007
I-II	47	29	18		32	15	
III-IV	19	4	15		6	13	
Histological grade				0.021			< 0.001
Low	42	25	17		32	10	
Moderate/advanced	24	8	18		6	18	
Lymph node metastasis				0.017			0.029
No	45	27	18		30	15	
Yes	21	6	15		8	13	

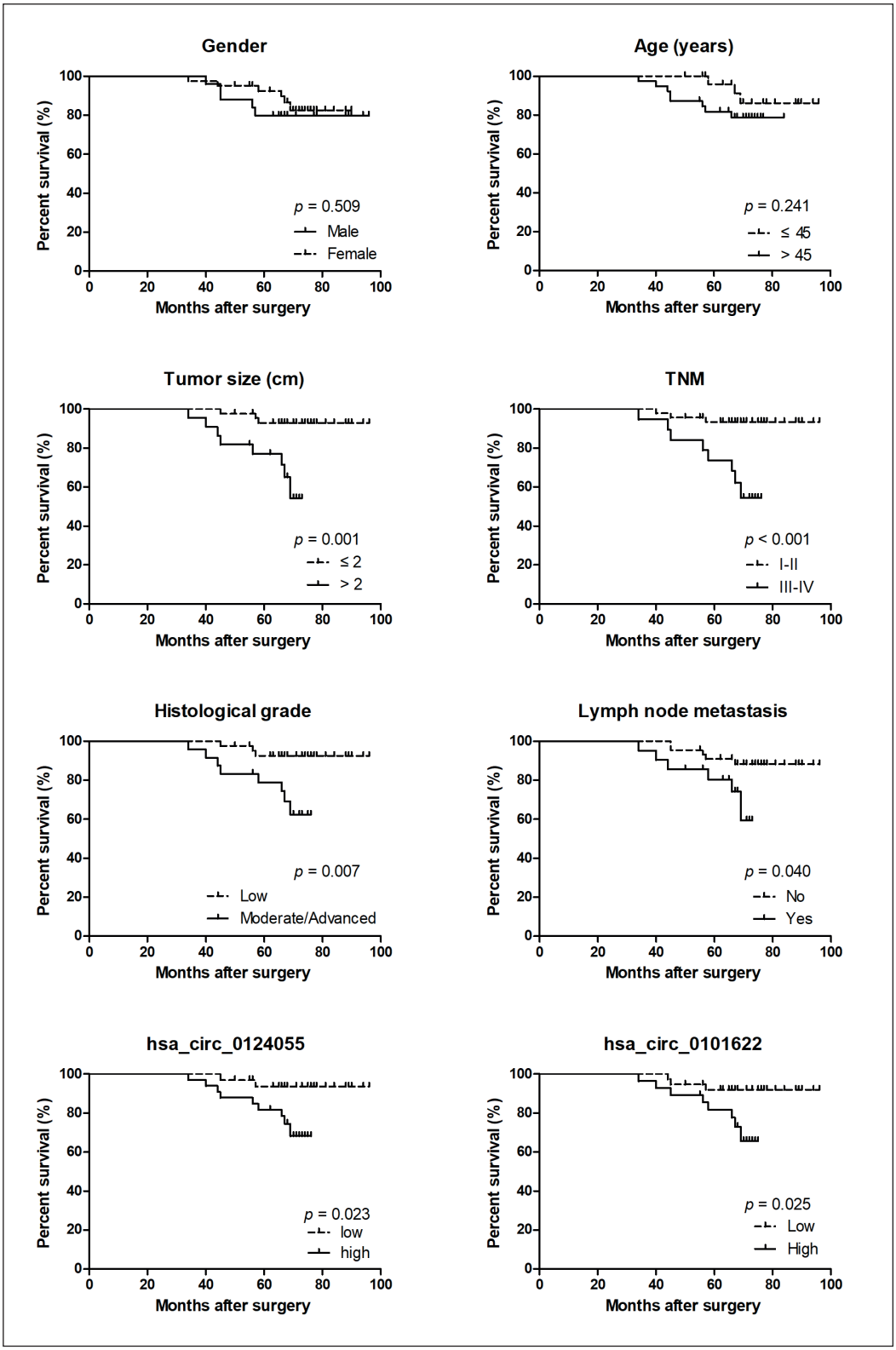

Figure 3. The association between physiopathological parameters and overall survival of thyroid cancer patients. Kaplan-Meier method with the log-rank test is applied to evaluate whether gender, age, tumor size, TNM stage, histological grade, lymph node metastasis, hsa_circ_0124055 and hsa_circ_0101622 expression levels are associated with overall survival of thyroid cancer patients.

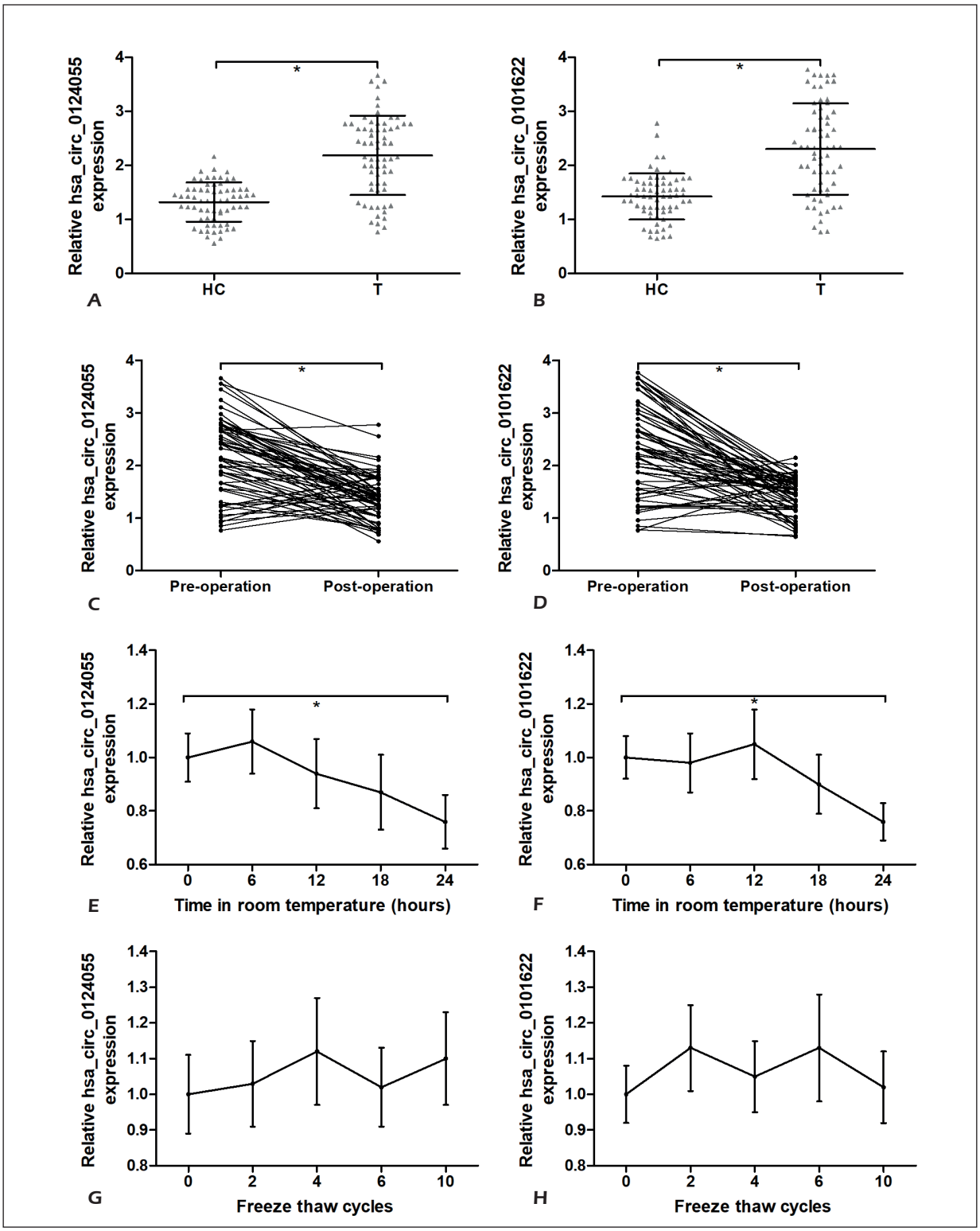

Figure 4. Hsa_circ_0124055 and hsa_circ_0101622 expression levels were up-regulated in the plasma of thyroid cancer patients. RT-PCR analysis is performed to measure the expression levels of hsa_circ_0124055 (**A**) and hsa_circ_0101622 (**B**) in the plasma of thyroid cancer patients (n = 66) and healthy subjects (n = 66). RT-PCR analysis is performed to measure the expression levels of hsa_circ_0124055 (**C**) and hsa_circ_0101622 (**D**) in the plasma of thyroid cancer patient before and 14 days after surgery. The stability of hsa_circ_0124055 and hsa_circ_0101622 under room temperature (**E** and **F**) and freeze-thaw conditions (**G** and **H**) was determined using RT-qPCR. *p<0.05.

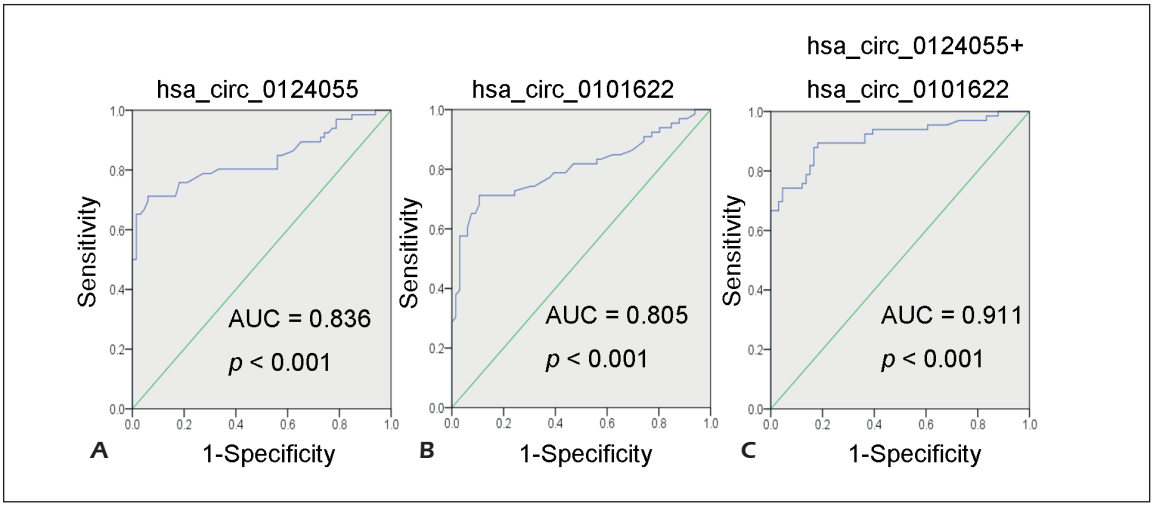

Figure 5. Hsa_circ_0124055 and hsa_circ_0101622 can serve as diagnostic biomarkers for T thyroid cancer screening. ROC curves and AUC are used to assess the diagnostic value of plasma hsa_circ_0124055 (**A**), hsa_circ_0101622 (**B**) or hsa_circ_0124055 combined with hsa_circ_0101622 (**C**) as diagnostic biomarkers of thyroid cancer.

hsa_circ_0101622 might function as oncogenes in the progression of thyroid cancer. First, the expression levels of hsa_circ_0124055 and hsa_circ_0101622 were explored in a normal thyroid follicular epithelium cell line (Nthy-ori3-1) and four thyroid cancer cell lines (K-1, TPC-1, B-CPAP and CAL-62). As expected, hsa_circ_0124055 and hsa_circ_0101622 expression levels were significantly increased in thyroid cancer cell lines compared with those in normal Nthy-ori3-1 cells (Figure 6A). Next, specific siRNAs were designed to silence the expression of hsa_circ_0124055 and hsa_circ_0101622 *in vitro*. After transfection with si-0124055 or si-0101622 into K-1 and TPC-1 cells, the proliferation of thyroid cancer cells was significantly inhibited, and cell apoptosis was significantly elevated compared with those of cells transfection with si-Con (Figure 6B and 6C). Notably, a combination of si-0124055 and si-0101622 showed a synergistic effect to inhibit cell proliferation and induce apoptosis *in vitro*.

Knockdown of Hsa_circ_0124055 and Hsa_circ_0101622 Inhibited Thyroid Cancer Cell Growth In Vivo

To determine the pro-proliferative activity of hsa_circ_0124055 and hsa_circ_0101622 *in vivo*, si-0124055 or si-0101622 was transfected into TPC-1 cells to suppress the expression of hsa_circ_0124055 or hsa_circ_0101622. Next, transfected TPC-1 cells (1×10^7/0.1 mL) were implanted subcutaneously into 4-week-old BALB/c nude mice, and tumor growth was evaluated every week for 5 weeks. Both tumor volume and weight were significantly inhibited by si-0124055 or si-0101622 transfection. We also found that the inhibitory effect of si-0124055 combined with si-0101622 on tumor volume and weight was significantly better than that of si-0124055 or si-0101622 transfection alone (Figure 7A and 7B).

Discussion

During the last decade, nucleic acids in the cell-free plasma or serum were detectable and

Table III. Performance of hsa_circ_0124055 and hsa_circ_0101622 in the differential diagnosis PTC from healthy controls.

	AUC	p-value	95% CI		Sensitivity	Specificity	Youden index	Cutoff point
			Lower	Upper				
Hsa_circ_0124055	0.836	< 0.001	0.763	0.908	0.712	0.939	0.652	1.805
Hsa_circ_0101622	0.805	< 0.001	0.727	0.883	0.712	0.894	0.606	1.825
Combined	0.911	< 0.001	0.859	0.962	0.894	0.818	0.712	2.869

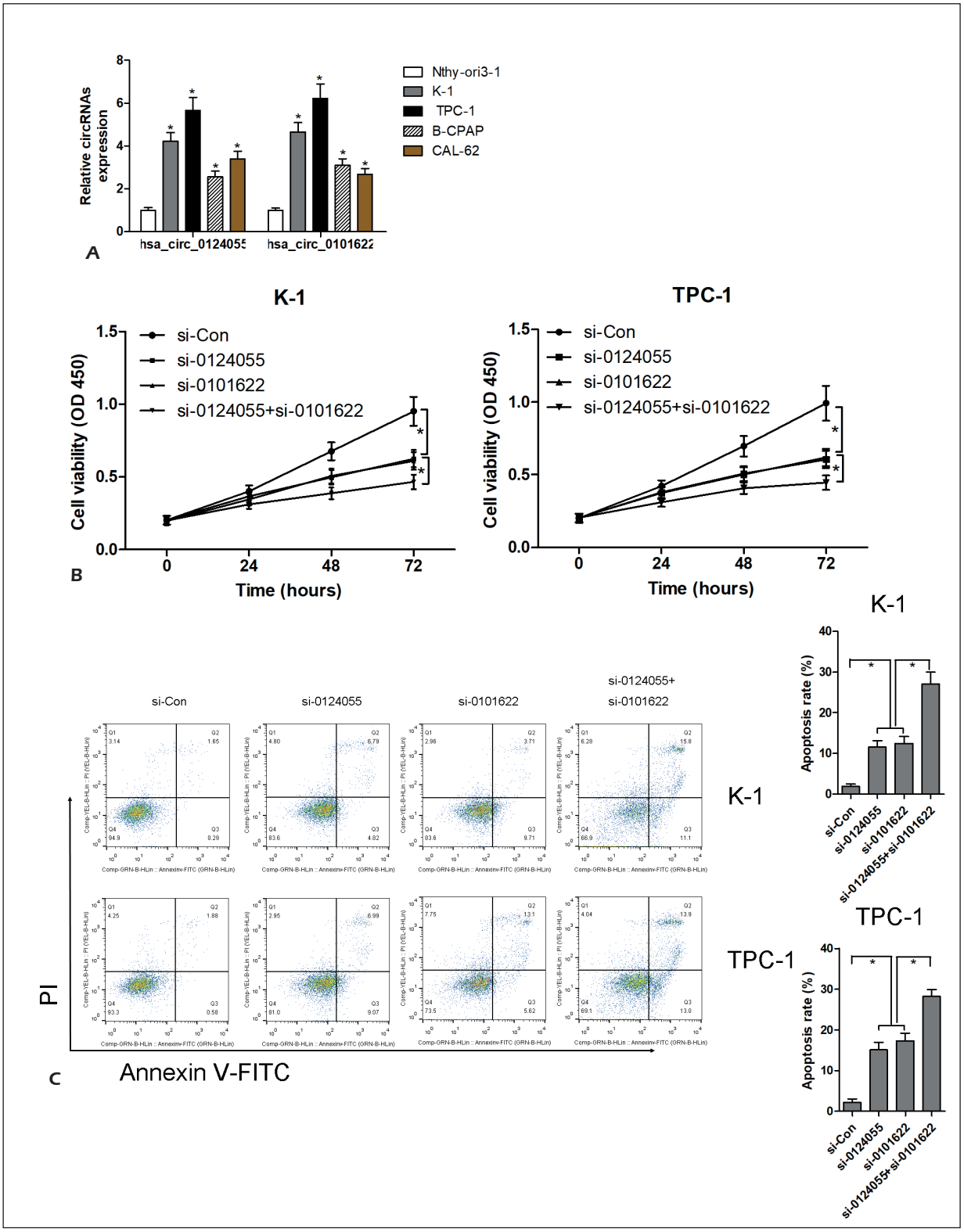

Figure 6. Knockdown of hsa_circ_0124055 and hsa_circ_0101622 led to thyroid cancer cell growth blockage and apoptosis. The expression levels of hsa_circ_0124055 and hsa_circ_0101622 were measured in a normal thyroid follicular epithelium cell line (Nthy-ori3-1) and four thyroid cancer cell lines (K-1, TPC-1, B-CPAP and CAL-62) using RT-qPCR (**A**). After transfection with si-Con, si-0124055 or si-0101622 into K-1 and TPC-1 cells, cell viability (**B**) and apoptosis (**C**) were detected using CCK8 and Annexin V-FITC/PI double staining, respectively. *p<0.05.

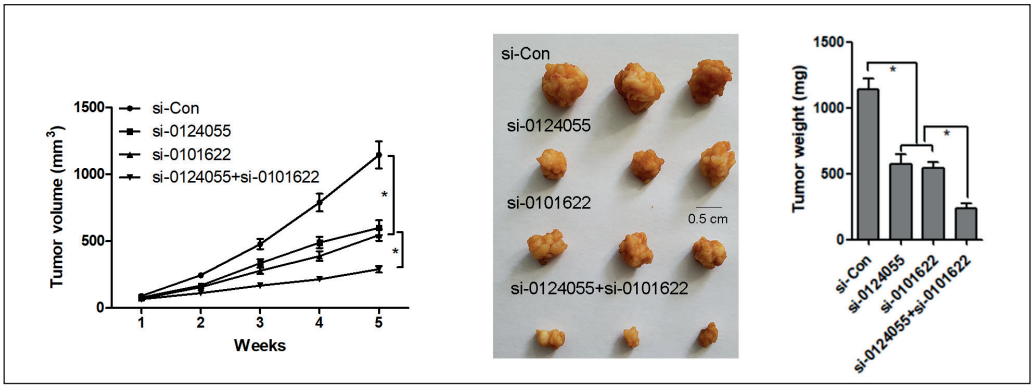

Figure 7. Knockdown of hsa_circ_0124055 and hsa_circ_0101622 inhibited thyroid cancer cell growth in vivo. Si-Con, si-0124055 or si-0101622 was transfected into TPC-1 cells (1 × 107 cells/0.1 mL), and then cells were implanted subcutaneously into 4-week-old BALB/c nude mice, and tumor volume (**A**) or weight (**B**) were evaluated after 5 weeks of cell implantation. *p<0.05.

therefore supposed to be utilized as noninvasive biomarkers for the diagnosis of cancers[22,23]. Although numerous miRNAs and lncRNAs have been highlighted as novel tumor indicators for cancerous prognosis prediction and diagnosis[24,25], the role of plasma circRNAs in the prognosis and diagnosis of thyroid cancer remains unclear.

In our study, thyroid cancer-related circRNAs screening was explored using high-throughput sequencing analysis in five pairs of thyroid cancer and adjacent non-tumor tissues to filtrate differentially expressed circRNAs. The top six abnormally expressed circRNAs of interest were then screened out as candidate biomarkers. Among these circRNAs, only hsa_circ_0124055 and hsa_circ_0101622 were significantly increased in thyroid cancer tissues compared with those in adjacent non-tumor tissues. Therefore, hsa_circ_0124055 and hsa_circ_0101622 were subjected to RT-qPCR validation. As expected, RT-qPCR data were consistent with the results from high-throughput sequencing. Ultimately, hsa_circ_0124055 and hsa_circ_0101622 were established as potential biomarkers for further study. In both tumor tissues and plasma of thyroid cancer patients, a significant increase in hsa_circ_0124055 and hsa_circ_0101622 expression level was validated by RT-qPCR. First, we corroborated that patients with high hsa_circ_0124055 or hsa_circ_0101622 expression exhibited shorter overall survival. Our findings provided strong evidence that plasma hsa_circ_0124055 and hsa_circ_0101622 could be used as diagnostic markers for thyroid cancer. Furthermore, hsa_circ_0124055 combined with hsa_circ_0101622 could provide a more powerful diagnostic value than hsa_circ_0124055 or hsa_circ_0101622 alone.

Novel circRNAs that can predict prognosis and improve clinical diagnosis of thyroid cancer. Yao et al[15] have reported that hsa_circ_0058124 is upregulated in 68.48% (63/92) of thyroid cancer tissues and correlated with unfavorable prognosis, including extrathyroidal extension, large tumor size, advanced stage, lymph node metastasis, and distant metastasis. However, the association between hsa_circ_0058124 expression and overall survival has not been delineated in this study[15]. Lan et al[26] have demonstrated that the downregulation of hsa_circ_0137287 is correlated with aggressive clinicopathologic characteristics, such as extrathyroidal extension, lymph node metastasis, advanced T stage, and larger tumor size, in thyroid cancer patients, and hsa_circ_0137287 exhibits a potential diagnostic value in thyroid cancer (AUC = 0.897, 95% CI: 0.8452-0.9494, $p < 0.001$). Similarly, our findings discovered that the upregulation of hsa_circ_0124055 or hsa_circ_0101622 in thyroid cancer tissues was associated with poor clinicopathological parameters and overall survival. Moreover, plasma hsa_circ_0124055 (AUC = 0.836, 95% CI: 0.763-0.908, $p < 0.001$) and hsa_circ_0101622 (AUC = 0.805, 95% CI: 0.727-0.883, $p < 0.001$) showed a high-efficiency diagnosis performance for distinguishing thyroid cancer from healthy subjects.

Our results also validated that circulating hsa_circ_0124055 and hsa_circ_0101622 were remarkably stable in room temperature and freeze-thaw conditions. Therefore, stable property made it possible for them to serve as diagnostic markers in clinical practice.

Numerous circRNAs have been corroborated to manage cancer cell growth *in vivo* and *in vitro*. CircPTN accelerates glioma cell proliferation *in vitro* and *in vivo via* promoting the transition of the G1-S phase in U87 and U251 cells[27]. Inversely, circRNA CBL.11 inhibits cell proliferation in colorectal cancer cells by sponging miR-6778-5p[28]. In our study, we also found that the knockdown of hsa_circ_0124055 or hsa_circ_0101622 expression led to the decline of the proliferating rate of thyroid cancer cells. Notably, the inhibition of hsa_circ_0124055 or hsa_circ_0101622 simultaneously exhibited a significantly higher proliferating rate than the silencing of hsa_circ_0124055 or hsa_circ_0101622 alone.

However, some limitations still existed in our study. For example, the precise mechanism whereby circRNAs are released into blood remained largely unknown, and the underlying molecular mechanisms of hsa_circ_0124055 and hsa_circ_0101622 had not been expounded in the initiation and progression of thyroid cancer.

Conclusions

Our findings indicated that hsa_circ_0124055 and hsa_circ_0101622 could be utilized as prognostic and diagnostic biomarkers for thyroid cancer. Of note, a combination of hsa_circ_0124055 and hsa_circ_0101622 showed a higher positive diagnostic rate of thyroid cancer.

Funding

This research was supported by the National Natural Science Foundation of China (Grant no. 81360398).

Conflict of Interests

The authors declare they have no conflict of Interest.

References

1) Bray F, Ferlay J, Soerjomataram I, Siegel RL, Torre LA, Jemal A. Global cancer statistics 2018: GLOBOCAN estimates of incidence and mortality worldwide for 36 cancers in 185 countries. CA Cancer J Clin 2018; 68: 394-424.
2) Chen W, Zheng R, Baade PD, Zhang S, Zeng H, Bray F, Jemal A, Yu XQ, He J. Cancer statistics in China, 2015. CA Cancer J Clin 2016; 66: 115-132.
3) Abdullah MI, Junit SM, Ng KL, Jayapalan JJ, Karikalan B, Hashim OH. Papillary thyroid cancer: genetic alterations and molecular biomarker investigations. Int J Med Sci 2019; 16: 450-460.
4) Cheng CJ, Bahal R, Babar IA, Pincus Z, Barrera F, Liu C, Svoronos A, Braddock DT, Glazer PM, Engelman DM, Saltzman WM, Slack FJ. MicroRNA silencing for cancer therapy targeted to the tumour microenvironment. Nature 2015; 518: 107-110.
5) Kleaveland B, Shi CY, Stefano J, Bartel DP. A network of noncoding regulatory RNAs acts in the mammalian brain. Cell 2018; 174: 350-362.e317.
6) Piwecka M, Glazar P. Loss of a mammalian circular RNA locus causes miRNA deregulation and affects brain function. Science 2017; 357: pii: eaam8526.
7) Yan B, Zhang W, Mao XW, Jiang LY. Circular RNA ciRS-7 correlates with advance disease and poor prognosis, and its down-regulation inhibits cells proliferation while induces cells apoptosis in non-small cell lung cancer. Eur Rev Med Pharmacol Sci 2018; 22: 8712-8721.
8) Conn SJ, Pillman KA, Toubia J, Conn VM, Salmanidis M, Phillips CA, Roslan S, Schreiber AW, Gregory PA, Goodall GJ. The RNA binding protein quaking regulates formation of circRNAs. Cell 2015; 160: 1125-1134.
9) Kristensen LS, Hansen TB, Veno MT, Kjems J. Circular RNAs in cancer: opportunities and challenges in the field. Oncogene 2018; 37: 555-565.
10) Huang X, Zhang W, Shao Z. Prognostic and diagnostic significance of circRNAs expression in hepatocellular carcinoma patients: a meta-analysis. Cancer Med 2019; 8: 1148-1156.
11) Zhu YJ, Zheng B, Luo GJ, Ma XK, Lu XY, Lin XM, Yang S, Zhao Q, Wu T, Li ZX, Liu XL, Wu R, Liu JF, Ge Y, Yang L, Wang HY, Chen L. Circular RNAs negatively regulate cancer stem cells by physically binding FMRP against CCAR1 complex in hepatocellular carcinoma. Theranostics 2019; 9: 3526-3540.
12) Jiang XM, Li ZL, Li JL, Xu Y, Leng KM, Cui YF, Sun DJ. A novel prognostic biomarker for cholangiocarcinoma: circRNA Cdr1as. Eur Rev Med Pharmacol Sci 2018; 22: 365-371.
13) Peng N, Shi L, Zhang Q, Hu Y, Wang N, Ye H. Microarray profiling of circular RNAs in human papillary thyroid carcinoma. PLoS One 2017; 12: e0170287.
14) Liu Q, Pan LZ, Hu M, Ma JY. Molecular network-based identification of circular RNA-associated ceRNA network in papillary thyroid cancer. Pathol Oncol Res 2019. doi: 10.1007/s12253-019-00697-y. [Epub ahead of print].
15) Yao Y, Chen X, Yang H, Chen W, Qian Y, Yan Z, Liao T, Yao W, Wu W, Yu T, Chen Y, Zhang Y. Hsa_circ_0058124 promotes papillary thyroid cancer tumorigenesis and invasiveness through the NOTCH3/GATAD2A axis. J Exp Clin Cancer Res 2019; 38: 318.
16) Liu W, Zhao J, Jin M, Zhou M. circRAPGEF5 Contributes to papillary thyroid proliferation and met-

astatis by regulation miR-198/FGFR1. Mol Ther Nucleic Acids 2019; 14: 609-616.

17) Bi W, Huang J, Nie C, Liu B, He G, Han J, Pang R, Ding Z, Xu J, Zhang J. CircRNA circRNA_102171 promotes papillary thyroid cancer progression through modulating CTNNBIP1-dependent activation of beta-catenin pathway. J Exp Clin Cancer Res 2018; 37: 275.

18) Kim D, Pertea G, Trapnell C, Pimentel H, Kelley R, Salzberg SL. TopHat2: accurate alignment of transcriptomes in the presence of insertions, deletions and gene fusions. Genome Biol 2013; 14: R36.

19) de Hoon MJ, Imoto S, Nolan J, Miyano S. Open source clustering software. Bioinformatics 2004; 20: 1453-1454.

20) Livak KJ, Schmittgen TD. Analysis of relative gene expression data using real-time quantitative PCR and the 2(-Delta Delta C(T)) method. Methods 2001; 25: 402-408.

21) Tong YS, Wang XW, Zhou XL, Liu ZH, Yang TX, Shi WH, Xie HW, Lv J, Wu QQ, Cao XF. Identification of the long non-coding RNA POU3F3 in plasma as a novel biomarker for diagnosis of esophageal squamous cell carcinoma. Mol Cancer 2015; 14: 3.

22) Jiang P, Chan KCA, Lo YMD. Liver-derived cell-free nucleic acids in plasma: Biology and applications in liquid biopsies. J Hepatol 2019; 71: 409-421.

23) Tolle A, Blobel CC, Jung K. Circulating miRNAs in blood and urine as diagnostic and prognostic biomarkers for bladder cancer: an update in 2017. Biomark Med 2018; 12: 667-676.

24) Mahmoudian-Sani MR, Jalali A, Jamshidi M, Moridi H, Alghasi A, Shojaeian A, Mobini GR. Long non-coding RNAs in thyroid cancer: implications for pathogenesis, diagnosis, and therapy. Oncol Res Treat 2019; 42: 136-142.

25) Rezaei M, Khamaneh AM, Zarghami N, Vosoughi A. Evaluating pre- and post-operation plasma miRNAs of papillary thyroid carcinoma (PTC) patients in comparison to benign nodules. BMC Cancer 2019; 19: 690.

26) Lan X, Cao J, Xu J, Chen C, Zheng C, Wang J, Zhu X, Zhu X, Ge M. Decreased expression of hsa_circ_0137287 predicts aggressive clinicopathologic characteristics in papillary thyroid carcinoma. J Clin Lab Anal 2018; 32: e22573.

27) Chen J, Chen T, Zhu Y, Li Y, Zhang Y, Wang Y, Li X, Xie X, Wang J, Huang M, Sun X, Ke Y. circPTN sponges miR-145-5p/miR-330-5p to promote proliferation and stemness in glioma. J Exp Clin Cancer Res 2019; 38: 398.

28) Li H, Jin X, Liu B, Zhang P, Chen W, Li Q. CircRNA CBL.11 suppresses cell proliferation by sponging miR-6778-5p in colorectal cancer. BMC Cancer 2019; 19: 826.